1 November 2001

ELSEVIER

Optics Communications 198 (2001) 439–445

OPTICS COMMUNICATIONS

www.elsevier.com/locate/optcom

Parametric signal regeneration

G.R. Collecutt *, P.D. Drummond

Department of Physics, The University of Queensland, Qld 4072, Australia

Received 28 November 2000; received in revised form 17 May 2001; accepted 8 August 2001

Abstract

We present an ultra-high bandwidth all-optical digital signal regeneration device concept utilising non-degenerate parametric interaction in a one-dimensional waveguide. Performance is analysed in terms of re-amplification, re-timing, and re-shaping (including centre frequency correction) of time domain multiplexed signals. Bandwidths of 10–100 THz are achievable. © 2001 Published by Elsevier Science B.V.

PACS: 42.65.P; 42.65.T; 42.79.T

Keywords: Parametric; Non-linear; Optical; Logic; Regeneration

Current technology for regeneration of time domain multiplexed signals in an optical fibre communications network falls well short of utilising the full information bandwidth available within a fibre. The erbium doped fibre laser is capable of re-amplification of signals with a bandwidth of order 1 THz, while re-timing and re-shaping are still performed electronically by receiving the signals and re-sending them. Since the current bandwidth of electronics is only of order 10 GHz we find a present trend toward using wavelength division multiplexing, or WDM, to utilise the available bandwidth. In this paper we present an all-optical digital signal regeneration device concept utilising non-degenerate parametric interaction in a one-dimensional waveguide. Given that parametric logic can operate on femtosecond time scales [1], this device is entirely capable of achieving 10–100 THz bandwidth in one channel. This is close to the maximum available bandwidth in an optical fibre.

The concept is this: a weak signal pulse within a fibre is mixed with a stronger concurrent second harmonic (or near) pump pulse via a fibre coupler. The superposition then propagates into a one-dimensional $\chi^{(2)}$ waveguide cut for an appropriate type of parametric interaction. The weak signal pulse seeds the down-conversion of the pump pulse, so that by the end of the $\chi^{(2)}$ waveguide most of the pump energy has been down converted into the signal and idler fields. The regenerated signal pulse may then be isolated using a wavelength filter (and also a polarising filter if type II interactions are used) and allowed to continue to propagate in the communication network.

The key here is that the interaction is non-degenerate, thus requiring the interplay between three distinct fields. This way two fields with a random relative phase may be present initially,

* Corresponding author. Tel.: +61-7-3365-3405; fax: +61-7-3365-1242.

E-mail address: collecug@physics.uq.edu.au (G.R. Collecutt).

0030-4018/01/$ - see front matter © 2001 Published by Elsevier Science B.V.
PII: S0030-4018(01)01538-3

and the third field is generated with the necessary phase for energy to flow into it (whether or not it maintains this phase is a matter of phase matching). If using a type I interaction this would require that the signal and idler fields be non-degenerate in frequency space, which for this concept would require the pump field to be de-tuned from the second harmonic of the signal pulse. However, with type II interaction the signal and idler fields are already non-degenerate since they have orthogonal polarisations, and may have the same frequency if so desired.

Degenerate type I interaction on the other hand only involves two fields, which here are both present at the outset. If the relative initial phase between these fields is random, it is possible (at the extreme) for the pump field to absorb the signal. It is perhaps feasible to control the relative phase between the initial signal and pump fields, which would enable degenerate type I interaction, but for now this report focuses on the non-degenerate interaction.

The idea of using seeded parametric down-conversion to perform all-optical regeneration of ultra-short signal pulses appears to have been first introduced by Akhmanov [2], and then studied in more detail by Berishev [3] in 1989 for type I interaction, with type II interaction by Indenbaum [4] a year later. In both cases the pump field was quasi-CW and the authors were primarily concerned with re-amplification of the signal pulse. More recently, related work was performed by Canva [5] and Fuerst [6]. In particular they both considered the formation of one-dimensional spatial solitons, and derived conclusions that include: (a) the existence of a threshold seed energy, below which linear amplification of the signal takes place and above which amplification saturates for several orders of magnitude of signal power, (b) that this threshold energy is related to the spatial overlap of the signal energy with the pump energy, (c) that the relative phase and polarisation of the seed is unimportant, and (d) that this behaviour is well suited to all-optical switching and regeneration schemes. Further, Di Trapani et al. [7] have demonstrated experimentally that it is possible to lower this threshold to that of vacuum fluctuations, thus amplifying the incoherent quantum noise to form a quadratic spatial solitary wave. In this report we now consider this process of seeded down-conversion as a temporal problem rather than a spatial one. We also make no reference to solitons or energy localisation effects of any form.

Eqs. (1) and (2) describe the $1+1$D non-degenerate parametric interaction in dimensionless coordinates (adapted from Ref. [8]):

$$\frac{\partial\phi_j}{\partial\xi} = \mathrm{i}\left(-\frac{1}{2}\frac{\partial^2}{\partial\tau^2}\phi_j + \phi^*_{3-j}\phi_3 \right); \quad j = 1,2, \tag{1}$$

$$\frac{\partial\phi_3}{\partial\xi} = \mathrm{i}\left(-\frac{\sigma}{2}\frac{\partial^2}{\partial\tau^2}\phi_3 + \phi_1\phi_2 \right), \tag{2}$$

in which we have assumed the dispersion to be the same for signal and idler modes, and the relative dispersion of the pump mode given by σ. This theory is somewhat idealised in that it neglects phase velocity and group velocity mismatch, higher order dispersion, Raman scattering, and any possible effects due to non-linear dispersion. Nevertheless, it still embodies the principle of the interaction. The variable transformations are given by (adapted from Ref. [9]):

$$\phi_i = \frac{\Phi_i}{\Phi_0}; \quad \xi = \frac{z}{z_0}; \quad \tau = \frac{t - z/v_\mathrm{g}}{t_0}, \tag{3}$$

where $|\Phi_i|^2$ is the photon flux in mode i, $|\Phi_0|^2$ is a reference photon flux, z is the direction of propagation, t is time, and v_g is the group velocity of the three fields. Eqs. (4) and (5) define the scalars t_0, and Φ_0:

$$t_0^2 = z_0|\beta_2|; \quad \Phi_0 z_0 \chi = 1, \tag{4}$$

$$\chi = \chi^{(2)}\epsilon_0\left(\frac{\hbar k_1 k_2 k_3}{2\epsilon_1\epsilon_2\epsilon_3}\right)^{1/2}\int u_1 u_2 u_3^* \,\mathrm{d}x\,\mathrm{d}y, \tag{5}$$

where k_i and ϵ_i are the wave number and electric permittivity respectively of mode i within the $\chi^{(2)}$ media. β_2 is the dispersion at the signal and idler wavelengths, $\chi^{(2)}$ is the appropriate element of the quadratic non-linearity tensor, and u_i the transverse mode functions. Lastly z_0 is an arbitrary length scalar, which, in accordance with Eq. (4), represents the dispersion length for a Gaussian pulse of width t_0 at its waist.

To investigate the interaction, numerical simulations were performed using a split-step semi-

implicit integration method [10] on a one-dimensional lattice. [1] Figs. 1 and 2 display the results for the evolution of the signal and pump fields respectively for the case of $\sigma = 1$; the ordinate in each case being the field power.

It can be seen in Fig. 2 that the pump field is depleted with nearly half of its energy transferring to the signal field, as seen in Fig. 1. An equal quantity of energy is transferred to the idler field in much the same manner. The initial pulse profiles are Gaussian, as given in Eq. (6):

$$\phi_i = \alpha_i \exp\left[-\left(\frac{\tau - \Delta\tau_i}{\tau_{0_i}}\right)^2 + \mathrm{i}\Delta\omega_i\tau\right], \tag{6}$$

where $\Delta\tau_i$ and $\Delta\omega_i$ are the time and frequency offsets for the three pulses, and where

$$\tau_{0_i} = \sqrt{\frac{2}{\ln(2)}}\tau_{\mathrm{H}_i}; \quad \alpha_i = \sqrt{\frac{\mathscr{E}_i}{\sqrt{\frac{\pi}{2}}\tau_{0_i}}}, \ i = 1, 2; \qquad \alpha_3 = \sqrt{\frac{\mathscr{E}_3}{2\sqrt{\frac{\pi}{2}}\tau_{0_3}}}. \tag{7}$$

The total energy for the pump pulse was $\mathscr{E}_3 = 312$ in the dimensionless units. Its half width at half maximum was $\tau_{\mathrm{H}_3} = 0.5$, and it was centred with $\Delta\tau_3 = \Delta\omega_3 = 0$. The input signal pulse was similar, save that its energy, $\mathscr{E}_1$, was at -33 dB with respect to the input pump energy. The idler field was initialised to zero (i.e. $\mathscr{E}_2 = 0$).

The energy, time and frequency centres, and an equivalent half width half maximum (based on Gaussian second moment of area) of each pulse may also be found at any point during the interaction using Eqs. (8)–(10)

$$\mathscr{E}_i(\xi) = \int \phi_i^*\phi_i \,\mathrm{d}\tau, \ \ i = 1, 2; \qquad \mathscr{E}_3(\xi) = 2\int \phi_3^*\phi_3 \,\mathrm{d}\tau, \tag{8}$$

$$\Delta\tau(\xi) = \frac{\int \tau\phi^*\phi \,\mathrm{d}\tau}{\int \phi^*\phi \,\mathrm{d}\tau}; \quad \Delta\omega(\xi) = \frac{\int \omega\phi^*\phi \,\mathrm{d}\omega}{\int \phi^*\phi \,\mathrm{d}\tau}, \tag{9}$$

[1] The software package developed for these simulations is called XMDS, and is available at http://www.physics.uq.edu.au/xmds, as also are the input scripts used for Figs. 1 and 2.

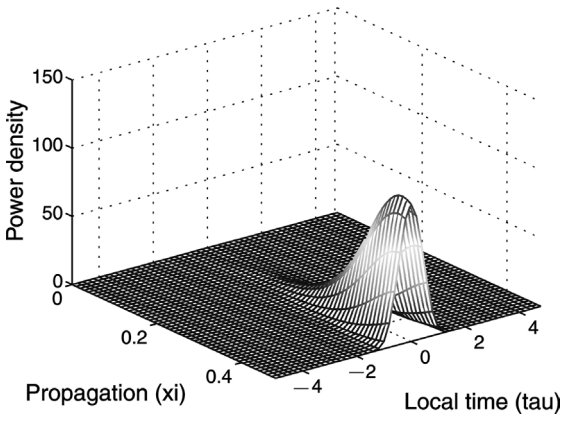

Fig. 1. Evolution of signal pulse.

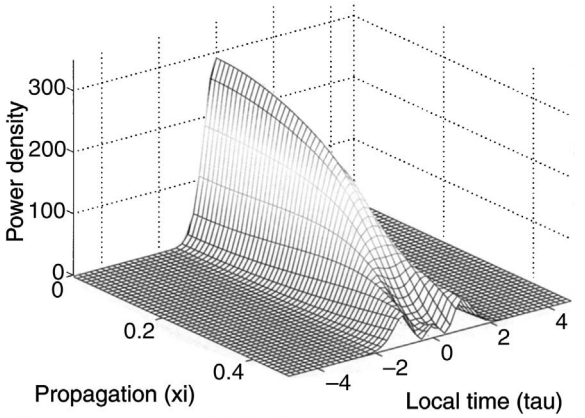

Fig. 2. Evolution of pump pulse.

$$\tau_{\mathrm{H}}(\xi) = \left[2\ln(2)\left(\frac{\int \tau^2\phi^*\phi \,\mathrm{d}\tau}{\int \phi^*\phi \,\mathrm{d}\tau} - (\Delta\tau)^2\right)\right]^{1/2}. \tag{10}$$

The resulting field energies and equivalent half widths for this simulation are shown in Figs. 3 and 4. The signal and idler energies grow exponentially while they remain small with respect to the pump pulse, but then the growth rounds off as the pump field is depleted. The growth of the idler pulse is proportional to the product of the signal and pump profiles, hence it initially develops a width which is smaller by a factor of $\sqrt{2}$. The width of the signal pulse decreases initially for the same reason. Eventually dispersion takes effect and the widths of both signal and idler pulses increase.

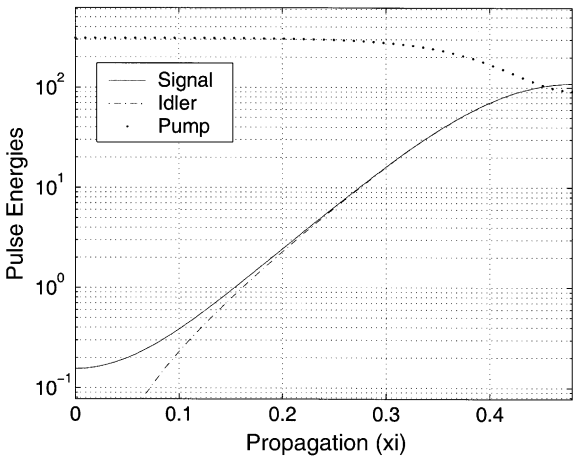

Fig. 3. Evolution of pulse energies.

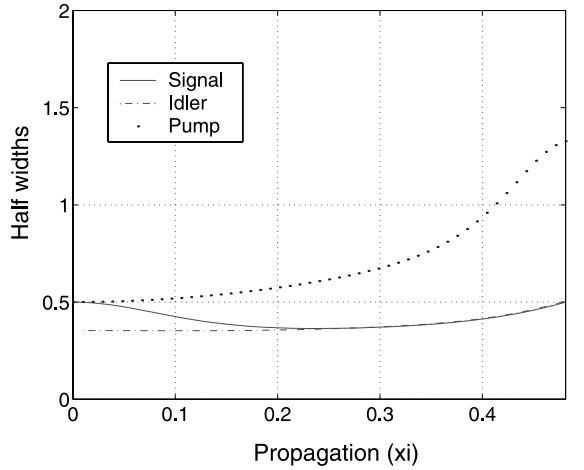

Fig. 4. Evolution of pulse widths.

Note the rapid increase in effective width of the pump pulse due to its central region being depleted. These two figures illustrate the two criteria that ultimately determine the necessary pump pulse energy and regeneration length. Firstly, the rate of energy growth of the signal pulse ought to be zero at the end of the interaction. This way small perturbations in the input signal pulse energy do not greatly affect the output energy. And secondly, the output signal pulse width ought to be the same as that of the nominal input signal pulse width. For the case of $\sigma = 1$ we find the necessary input pump pulse energy is 312 (in dimensionless units) and the matching regeneration length is $0.481 z_0$.

In order to evaluate the regeneration performance of this device we need to identify the parameters describing the signal pulse that are likely to need regeneration. Firstly, the energy of the signal pulse, $\mathscr{E}_1$, attenuates with propagation due to absorption, and the signal must be re-amplified. However, any form of amplifier adds noise to the signal, and so the shape of the pulse is degraded. This applies in the time domain, leading to timing error, $\Delta\tau_1$, and also in the frequency domain, leading to centre frequency error, $\Delta\omega_1$. Raman interactions within the fibre also lead to noise on the signal with similar results. Further, the dispersion characteristics of the fibre cause a centre frequency error to generate an associated timing error, and although this can be undone to some extent with dispersion correction and/or management, it is seldom completely recovered. Finally the pulse width will also be corrupted by the noise, hence the pulse width parameter, τ_{H_1}, is also a necessary descriptor.

Ideally, we would like to represent the regeneration as a function that maps the four variables, $\mathscr{E}_1$, $\Delta\tau_1$, $\Delta\omega_1$, and τ_{H_1}, from input to output. An empirical form for this function was derived by means of a least squares fit to the numerical simulation results over an $11 \times 11 \times 11 \times 11$ lattice spanning the input parameter ranges shown in Table 1. Variable products of up to third order were considered, yielding 35 terms and coefficients for each expression for the four variables. Such a four-dimensional function is not easy to represent graphically, and must be reduced to a relevant selection of two- and three-dimensional plots.

Analysis of the fitted coefficients revealed two main results. The first significant result was that the output energy and pulse width were primarily

Table 1
Variable default values and perturbation ranges

Variable	Minimum	Maximum	Default
$\mathscr{E}_1/\mathscr{E}_3$	−36 dB	−30 dB	−33 dB
$\Delta\tau_1$	−0.5	0.5	0
$\Delta\omega_1$	−0.5	0.5	0
τ_{H_1}	0.3	0.7	0.5

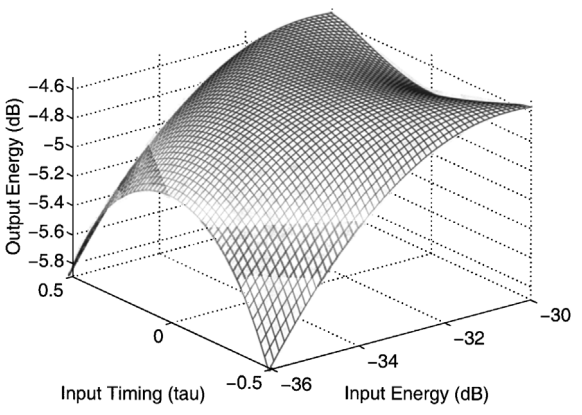

Fig. 5. Output signal pulse energy as a function of input signal energy and timing.

non-linear functions of input energy and timing, as shown in Figs. 5 and 6. As can be seen in Fig. 5, the output energy varies little over most of the input space, but begins to drop in the corners where the input energy is low and signal timing poor. This behaviour is undesirable and thus imposes a lower limit to the energy overlap between signal and pump pulses necessary for the amplification to saturate. Fig. 6 reveals that the output width rises slightly with higher input signal energies and low time errors. This is because the greater initial energy overlap causes the down-conversion process to deplete the pump pulse in its centre by the end of propagation, while energy

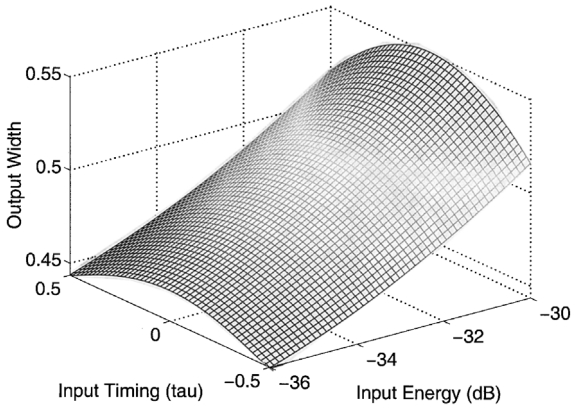

Fig. 6. Output signal pulse half width as a function of input signal energy and timing.

continues to down convert within the pulse wings, thus broadening the pulse. The output width also exhibits a sensitivity to the cross-product $(\Delta\tau_1)^2\tau_{H_1}$, in that this broadening effect is less pronounced when the input width is greater.

The second main result was that the output timing and frequency error were primarily linear functions of the input timing and frequency error, as shown in Eq. (11):

$$\begin{pmatrix} \Delta\tau_1 \\ \Delta\omega_1 \end{pmatrix}_{\text{out}} = \begin{bmatrix} a_{11} & a_{12} \\ a_{21} & a_{22} \end{bmatrix} \begin{pmatrix} \Delta\tau_1 \\ \Delta\omega_1 \end{pmatrix}_{\text{in}}. \tag{11}$$

A least squares fit over the domain $-0.5 \leqslant (\Delta\tau_1, \Delta\omega_1) \leqslant 0.5$ with $\mathscr{E}_1$ and τ_{H_1} set to the default values in Table 1 yielded the matrix elements $a_{11} = 0.1854$, $a_{12} = -0.0671$, $a_{21} = 0.0197$, and $a_{22} = 0.4820$. The a_{11} element has a slight dependence on the pulse width in that it decreases for a broader signal pulse. This is not that surprising since broadening the signal pulse shifts the overlap product between it and the pump pulse towards the centre of the pump pulse. The a_{21} and a_{22} elements are also dependent on the pulse width. This is because the pump pulse selectively amplifies only the frequency components of the signal pulse that propagate in step with it, hence the narrower the signal pulse, the greater the regeneration of the frequency error.

The linearity of the regeneration of $\Delta\tau_1$ and $\Delta\omega_1$ can be seen in Fig. 7, in which we show the evolution of the these parameters for 24 paths starting at points on the square bounding $-0.5 \leqslant (\Delta\tau_1, \Delta\omega_1) \leqslant 0.5$ (with $\mathscr{E}_1$ and τ_{H_1} set to the default values in Table 1) and ending on the inner quadrilateral.

We also consider the effect of varying the ratio of dispersions, σ. Increasing the dispersion of the pump mode relative to the signal mode results in the pump pulse broadening and lessening in intensity during the down-conversion process. This has the obvious effect of requiring a shorter interaction length and a greater energy of the pump pulse, as shown in Fig. 8, in order to meet the two output criteria mentioned earlier. Another strong effect occurs in that a broader pump pulse will be less effective at regenerating the timing of the signal pulse (since broadening the pump pulse shifts the overlap product between it and the signal pulse towards the centre of the signal pulse), as well as it

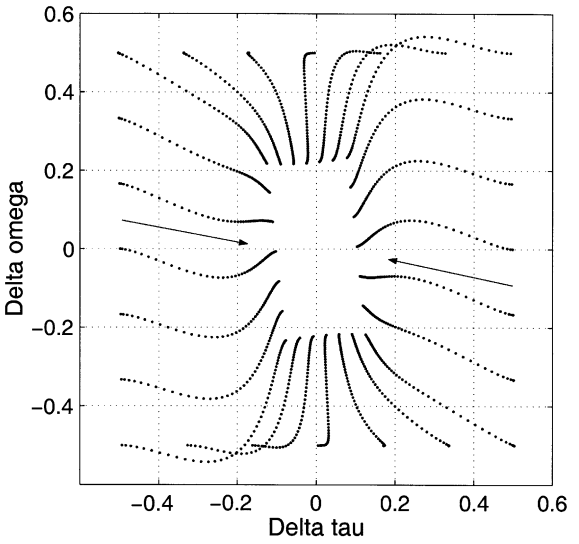

Fig. 7. Evolution of signal pulse time and frequency centres for $\sigma = 1.0$.

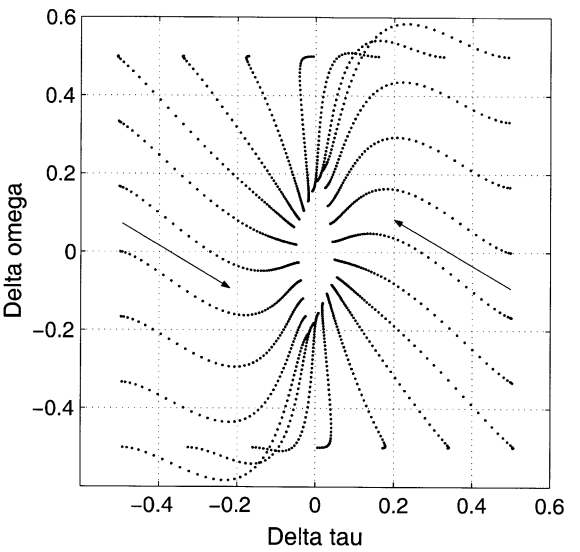

Fig. 9. Evolution of signal pulse time and frequency centres for $\sigma = 0$.

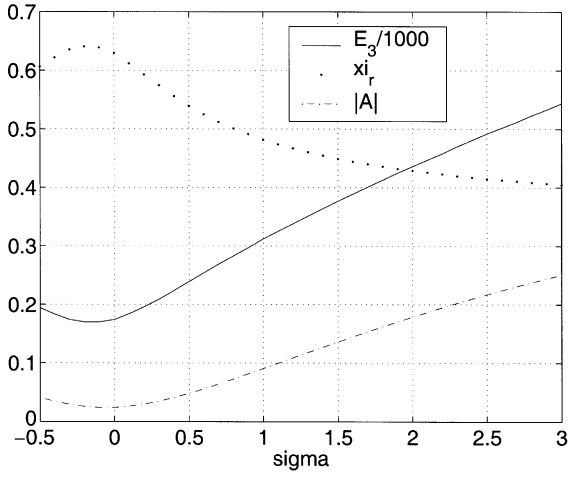

Fig. 8. Pump energy, regeneration length, and determinant of the **A** matrix versus σ.

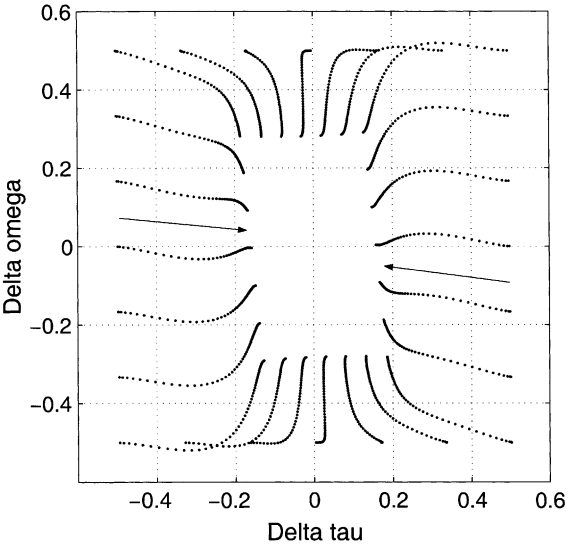

Fig. 10. Evolution of signal pulse time and frequency centres for $\sigma = 2.0$.

is less able to selectively amplify only the signal frequency components that are travelling in step with it. In other words the transfer matrix of Eq. (11) is highly dependent on σ. Similarly to Fig. 7, Figs. 9 and 10 show the evolution of $\Delta\tau_1$ and $\Delta\omega_1$ for the cases $\sigma = 0$ and $\sigma = 2$ respectively, while the determinant of the transfer matrix, **A**, which represents the ratio of areas between output and input domains, is also plotted in Fig. 8. As is evident the degree of regeneration is greatest for $\sigma = 0$ (where the pump pulse does not disperse) and decreases with increasing σ. The effect that σ has on the output energy is very small, while its effect

on the output width is more noticeable. When σ is small the pump pulse remains more intense, thus the tendency of higher energy simultaneous input pulses to broaden the output pulse (discussed earlier) becomes even more pronounced. As a result the variation in the output width seen in Fig. 6 monotonically decreases with increasing sigma.

Finally, we consider a couple of more practical aspects in regard to implementing this concept. Firstly the source of pump pulses must be synchronised, on average, with the signal data stream. This probably needs to be performed locally and all-optically in order to achieve THz data rates. One such idea for this has been put forward by Su et al. [11], in which they inject part of the signal into a fibre ring oscillator in order to synchronise the pulse train via a four wave mixing process. A second practical consideration is that very small pulses in the signal mode, i.e. noise, are linearly amplified according to their overlap with the pump pulse, while the gain of a genuine signal pulse is limited. Where multiple regeneration stages are implemented, noise will grow exponentially until comparable in power to the signal pulses. This is clearly an undesirable effect. One possible solution to this problem is to include a saturating absorber in the output line to attenuate small signals while allowing larger signals to pass with little attenuation.

In summary we have demonstrated numerically a device, utilising optical parametric non-linearity, which is capable of performing all-optical signal regeneration on a 10–100 THz bandwidth time domain multiplexed signal. Performance parameters were identified and the input output relationships determined. Output energy and pulse width were found to be primarily related to input energy and timing, while timing and frequency errors at output were found to be linearly related to their input values. The extent of regeneration of the latter two parameters was dependent on the ratio of dispersions between pump and signal modes. Further, it is not difficult to see that this device could also be used to de-multiplex both time domain and frequency domain multiplexed signals: time domain de-multiplexing could be performed by using the pump pulse to perform time channel selection, whereas frequency domain de-multiplexing could perhaps be performed by using the phase matching criterion to select the desired frequency channel.

Acknowledgements

The authors wish to acknowledge Gaetano Assanto for his comments and assistance.

References

[1] X. Liu, K. Beckwitt, F. Wise, Non-collinear generation of optical spatio-temporal solitons and application to ultrafast digital logic, Phys. Rev. E 61 (2000) 4722–4725.
[2] S.A. Akhmanov, V.A. Vysloukh, A.S. Chirkin, Optics of Femtosecond Laser Pulses, Nauka, Moscow, 1988 (in Russian).
[3] I.E. Berishev, A.V. Selishchev, A.S. Shcherbakov, Parametric regeneration of ultra-short light pulses in a medium with quadratic nonlinearity, Sov. Tech. Phys. Lett. 15 (1989) 614–616.
[4] D.M. Indenbaum, V.M. Sysuev, A.S. Shcherbakov, Nondegenerate parametric regeneration of ultra-short light pulses in crystals, Sov. Tech. Phys. Lett. 16 (1990) 540–542.
[5] M.T.G. Canva, R.A. Fuerst, S. Babiou, G.I. Stegeman, G. Assanto, Quadratic spatial soliton generation by seeded down conversion of a strong harmonic pump beam, Opt. Lett. 22 (1997) 1683–1685.
[6] R.A. Fuerst, M.T.G. Canva, G.I. Stegeman, G. Assanto, Robust generation, properties, and potential applications of quadratic spatial solitons generated by optical parametric amplification, Opt. Quant. Electron. 30 (1998) 907–921.
[7] P. Di Trapani, G. Valiulis, W. Chinaglia, A. Andreoni, Two-dimensional spatial solitary waves from travelling-wave parametric amplification of the quantum noise, Phys. Rev. Lett. 80 (1998) 265–268.
[8] P.D. Drummond, K.V. Kheruntsyan, H. He, Novel solitons in parametric amplifiers and atom lasers, J. Opt. B 1 (1999) 387–395.
[9] M.J. Werner, P.D. Drummond, Pulsed quadrature-phase squeezing of solitary waves in $\chi^{(2)}$ parametric waveguides, Phys. Rev. A 56 (1997) 1508–1518.
[10] P.D. Drummond, Central partial difference algorithms, Comput. Phys. Commun. 29 (1983) 211–225.
[11] Y. Su, L. Wang, A. Agarwal, P. Kumar, Wavelength tunable all-optical clock recovery using a fiberoptic parametric oscillator, Opt. Commun. 184 (2000) 151–156.